The oral bioavailability of a pleuromutilin antibiotic candidate is increased after co-administration with the CYP3A4 inhibitor ritonavir and the P-gp inhibitor zosuquidar formulated as amorphous solid dispersions

Petersen, Emilie Fynbo; Munch Rasmussen, Charlotte Laurfelt; Prabhala, Bala Krishna; Heidtmann, Christoffer Vogsen; Nielsen, Poul; Nielsen, Carsten Uhd

Published in:
International Journal of Pharmaceutics

DOI:
10.1016/j.ijpharm.2025.125397

Publication date:
2025

Document version:
Final published version

International Journal of Pharmaceutics 673 (2025) 125397

Contents lists available at ScienceDirect

International Journal of Pharmaceutics

journal homepage: www.elsevier.com/locate/ijpharm

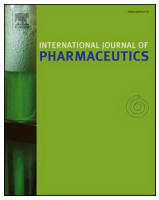

The oral bioavailability of a pleuromutilin antibiotic candidate is increased after co-administration with the CYP3A4 inhibitor ritonavir and the P-gp inhibitor zosuquidar formulated as amorphous solid dispersions

Emilie Fynbo Petersen [a], Charlotte Laurfelt Munch Rasmussen [b], Bala Krishna Prabhala [a], Christoffer Vogsen Heidtmann [a], Poul Nielsen [a], Carsten Uhd Nielsen [a,*]

[a] Department of Physics, Chemistry and Pharmacy, University of Southern Denmark, Campusvej 55, DK-5230 Odense M, Denmark
[b] Biomedical Laboratory, The Faculty of Health Sciences, University of Southern Denmark, Campusvej 55, DK-5230 Odense M, Denmark

ARTICLE INFO

Keywords:
Amorphous solid dispersion
Oral bioavailability
Pleuromutilin antibiotics
P-gp
CYP3A4
Solubility

ABSTRACT

The aim of the present work was to investigate if CYP-mediated metabolism or P-gp recognition were the main limitations to developing oral formulations of the pleuromutilin drug candidate CVH-174, **16**, and to subsequently increase the bioavailability through a formulation design based on amorphous solid dispersions (ASDs) containing either a CYP3A inhibitor or a P-gp inhibitor or both. ASDs were produced using HPMC-5 with ritonavir and zosuquidar as CYP3A4 and P-gp inhibitors, respectively, through freeze-drying. The ASDs were characterized using XRPD over time to assess the stability of the formulations. The oral bioavailability was investigated in Sprague-Dawley rats following either oral or intravenous (IV) dosing. The results showed that ritonavir could be supersaturated when formulated in an HPMC-5-based ASD, whereas HPMC-5-based ASDs could not increase the solubility of CVH-174 and zosuquidar. The ASD formulations remained stable for the period covering the experiments. *In vivo* IV dosing showed that CVH-174 was metabolized fast with a half-life of 0.15 h. The oral bioavailability of CVH-174 was low ~ 1 % and could not be increased by co-dosing with a P-gp inhibitor alone, whereas the CYP3A4 inhibitor ritonavir did increase the bioavailability. The combined co-administration of ritonavir- and zosuquidar-containing ASDs surprisingly increased CVH-174 bioavailability to around 18 %. In conclusion, the oral bioavailability of CVH-174 can be significantly increased through a formulation design encompassing an inhibitor of the CYP3A4 enzyme, and this holds great potential for the future development of an inherent metabolic labile pleuromutilin drug class.

1. Introduction

Antimicrobial resistance (AMR) is a major worldwide health concern, threatening public health systems, and demanding the development of new antibacterial medicine. If AMR continues at the current rate, it is predicted that 10 million people will die every year by 2050, being as high as the current number of deaths worldwide caused by cancer (Lennard et al., 2023; Murray et al., 2022; O'Neill, 2016; White and Hughes, 2019). This is caused by the rise in multidrug-resistant pathogens, decreased effectiveness of commonly prescribed antibiotics, as well as a lack of novel antibiotic drugs (Lennard et al., 2023; Murray et al., 2022). The fungal natural product pleuromutilin has since its identification in 1951 (Kavanagh et al., 1951, 1952) been used as a powerful scaffold from which to build potent semi-synthetic antibiotics. Commonly referred to as pleuromutilin conjugates, these have seen an increased focus due to their beneficial antibacterial properties, their unique mechanism of action, and their potency against challenging and multi-resistant infections caused by Gram-positive pathogens including *Staphylococcus aureus* (MRSA), *Streptococcus penumoniae*, and *Enterococcus faecium* (Goethe et al., 2019; Paukner and Riedl, 2017). The unique mechanism of action results in reduced cross-resistance with other antibiotic classes and a generally low resistance rate in the clinic, making pleuromutilin conjugates particularly valuable in the treatment of infections caused by resistant bacterial strains, and hence crucial for combating AMR (Eyal et al., 2016; Eyal et al., 2015; Goethe et al., 2019; Högenauer, 1975; Högenauer and Ruf, 1981; Long et al., 2006; Paukner and Riedl, 2017; Poulsen et al., 2001; Yan et al., 2006).

Currently, only one pleuromutilin, Lefamulin, is on the market for

* Corresponding author at: Department of Physics, Chemistry and Pharmacy, University of Southern Denmark, Campusvej 55, DK-5230 Odense M, Denmark.
E-mail address: cun@sdu.dk (C.U. Nielsen).

https://doi.org/10.1016/j.ijpharm.2025.125397
Received 10 January 2025; Received in revised form 18 February 2025; Accepted 21 February 2025
Available online 24 February 2025

systemic human use, approved for oral and intravenous administration for the treatment of community-acquired pneumonia (Adhikary et al., 2022; Falcó et al., 2020; Fong, 2023; Zhanel et al., 2021). Recently, a new drug-like pleuromutilin conjugate (**16**, CVH-174) was reported by Heidtmann et al. (2024). The compound displayed higher activity against Vancomycin-resistant *Enterococcus faecium* and *Streptococcus pneumoniae* than Lefamulin and importantly showed lowered affinity towards hERG (Lefamulin label warning). However, the oral bioavailability was only 0.3 % in mice and 6 % in pigs after oral administration of 30 mg/kg and 10 mg/kg CVH-174 2HCl, respectively (Heidtmann et al., 2024). Since CVH-174 was shown to be both a P-gp and a CYP3A4 substrate, the poor bioavailability could be a result of both limited intestinal absorption and extensive hepatic metabolism. Moreover, the aqueous solubility of CVH-174 was shown to be relatively low at 114 ± 14 μM (82 ± 10 μg/mL) and pH-dependent (Heidtmann et al., 2024). Since oral formulations are preferred, we hypothesized that increasing the solubility, as well as inhibiting P-gp and CYP3A4 could increase the oral bioavailability of CVH-174. To increase the aqueous solubility and potentially oral bioavailability of CVH-174, we formulated amorphous solid dispersions (ASD) which are highly employed for transiently increasing the aqueous solubility and bioavailability of poorly soluble and low oral bioavailable compounds (Hörter and Dressman, 2001; Pandi et al., 2020; Van den Mooter, 2012; Vo et al., 2013). We have recently shown that the oral bioavailability of P-gp substrates such as etoposide and paclitaxel can be increased by incorporating P-gp inhibitors such as either zosuquidar or encequidar into an ASD based on the HPMC-5 polymer (Nielsen et al., 2023; Petersen et al., 2024). This formulation approach significantly increased the oral bioavailability of etoposide by 25-fold and the relative bioavailability of paclitaxel by 24-fold (Nielsen et al., 2023; Petersen et al., 2024). This suggests that incorporating e.g. zosuquidar into an ASD with CVH-174 could increase the bioavailability if P-gp is, in fact, limiting the intestinal permeability of CVH-174. Similarly, studies have shown that co-dosing CYP3A4 inhibitors such as ritonavir can increase the oral bioavailability of drug substances being metabolized hepatically (Hammond et al., 2022; Hendrikx et al., 2013; Hendrikx et al., 2014; Loos et al., 2023, 2024; Owen et al., 2021; Zeldin and Petruschke, 2004). Therefore, the present study aimed to increase the oral bioavailability of the pleuromutilin candidate CVH-174 through a pharmaceutical formulation approach using transporter (P-gp) and enzyme (CYP3A4) inhibitors.

2. Materials and methods

2.1. Materials

The pleuromutilin antibiotic candidate, conjugate CVH-174 (**16**, Heidtmann et al., 2024), was synthesized in-house and converted to its dihydrochloride salt to increase the solubility as previously described by Heidtmann et al., 2024. From here on the compound is referred to as CVH-174 2HCl, whereas CVH-174 refers to the free base. Zosuquidar trihydrochloride salt (zosuquidar 3HCl) was acquired from MedKoo Biosciences (Morrisville, NC, USA). In the current publication "zosuquidar 3HCl" refers to the 3HCl salt and "zosuquidar" refers to the free base. Ritonavir and glycerol (for molecular biology, ≥99 %), were acquired from Merck Sigma Aldrich (St. Louis, USA). Ultra-pure water was obtained from an in-house Milli-Q water purification system (Merck Millipore, Burlington, MA, USA). Fasted State Simulated Intestinal Fluid V2 (FaSSIF-V2) powder was acquired from Biorelevant (London, UK) and prepared following the manufacturers' instructions. Methocel E5 Premium LV (Hydroxypropyl methylcellulose 5 (HPMC-5)) was a gift from Nutrition & Biosciences (New Milford, CT, USA). Acetonitrile (MeCN), methanol, sodium chloride, sodium hydroxide pellets, maleic acid, and *tert*-butanol were acquired from VWR Chemicals (Briare, France). Trifluoroacetic acid and acetic acid were acquired from Fisher Scientific (Loughborough, UK).

2.2. Solubility studies

2.2.1. Apparent solubility in FaSSIF-V2, pH 6.50, at 37 °C

2.00 mg CVH-174 2HCl, 3.00 mg ritonavir, and 3.00 mg zosuquidar 3HCl were weighed in a 5 mL glass vial, 5 mL plastic vial, and 5 mL glass vial, respectively, and then covered with aluminum foil. 3.00 mL FaSSIF-V2, pH 6.50, was added before the vials were placed in an oven at 20 rpm and 37 °C containing a rotator with a rotation of 20 rpm for 72 h. After 72 h there was an excess amount of the three compounds in the vials. 1 mL was aliquoted with a 1 mL Henke-Ject syringe (Henke Sass Wolf, Tuttlingen, DE) fitted with a Fine-Ject needle (Henke Sass Wolf, Tuttlingen, DE) and discarded; this was done twice to saturate the syringe. Another 1 mL was aliquoted and a Minisart® 0.2 μm filter (Regenerated Cellulose (RC 4), Sartorius Stedim, Stonehouse, UK) was applied to the syringe. The first 200 μL was used to saturate the filter and was thereafter discarded. The remaining approximately 800 μL was filtered, collected, and immediately diluted 1:1 with 2 % (v/v) acetic acid in acetonitrile (MeCN) into three separate HPLC vials (n = 3). The diluted samples were analyzed by HPLC-UV as described below (Section 2.3).

2.3. Simultaneous Quantification of CVH-174, zosuquidar and ritonavir by HPLC-UV

A Waters 2695 HPLC system connected to a Water 2487 Dual λ Absorbance Detector (Waters Corporation, MA, USA) was used to quantify CVH-174, zosuquidar, and ritonavir in the equilibrium solubility studies and the dissolution studies. The mobile phase consisted of 90 % (v/v) ultra-pure water and 10 % (v/v) MeCN containing 0.1 % (v/v) trifluoroacetic acid (TFA) (A) and 90 % (v/v) MeCN and 10 % (v/v) ultra-pure water containing 0.1 % (v/v) TFA (B). A reverse phase column (Nova-Pak® C18, 4 μm, 3.9x150mm, Waters, Milford, MA, USA) was applied and maintained at 45 °C. For CVH-174 the flow was 0.50 mL/min with a linear gradient from 0 % to 10 % B from 0 min to 2 min, and from 10 % to 60 % B from 2 min to 5 min. The flow was then constant at 60 % B from 5 min to 8 min. Samples of 10 μL, maintained at 15 °C, were injected and detected at 254 nm with a retention time of 2.70 min. For ritonavir, the flow was constant at 0.70 mL/min with an isocratic elution of 30 % A and 70 % B for a run time of 8 min. Samples of 10 μL, maintained at 15 °C, were injected and detected at 215 nm having a retention time of 2.25 min. For zosuquidar the flow was constant at 0.60 mL/min with 5 % B from 0 min to 0.5 min, and a linear gradient from 5 % to 95 % B from 0.5 min to 5.0 min. The flow was then reset to 5 % B at 6.0 min and constant at 5 % B from 6.0 min to 10.0 min. Samples of 10 μL, maintained at 15 °C, were injected and detected at 240 nm having a retention time of 8.20 min. Calibration curves of CVH-174, ritonavir, and zosuquidar were made by preparing samples from a 2.51 mM, 6.51 mM, and 10 mM stock solution in 1:2 ultra-pure water: MeCN, methanol, and methanol, respectively. The calibration curves of CVH-174, ritonavir, and zosuquidar ranged from 2.5 μM to 157.0 μM, 1 μM to 30 μM, and 5 μM to 100 μM, respectively, to determine the concentration of CVH-174, ritonavir, and zosuquidar in the respected sample. All calibration curves were prepared in 50 % B and thereafter diluted 1:1 with 2 % (v/v) acetic acid in MeCN. Fresh calibration curves were prepared before each respective sample batch and run.

2.4. Preparation of amorphous controls and amorphous solid dispersions

ASDs for *in vitro* studies were prepared by freeze-drying solutions of CVH-174, zosuquidar, or ritonavir in 70 % (v/v) tert–butanol in ultra–pure water with HPMC-5. The concentrations of the final individual solutions for the ASDs were 8.0 mg/mL, 2.1 mg/mL, 4.4 mg/mL, and 40 ± 0.12 mg/mL for CVH-174, zosuquidar, ritonavir, and HPMC-5, respectively. Solutions were prepared by magnetic stirring overnight to ensure complete dissolution. The CVH-174 solution was light orange, the ritonavir solution was clear, and the zosuquidar solution was light

yellow. The solutions were transferred to individual falcon tubes (Sarstedt, DE) and placed in a −80 °C freezer for at least 3 h before freeze-drying. The solutions were freeze-dried in a Heto Drywinner freeze-dryer (Model DW 1.0–110, Alleroed, DK). The main drying was performed over 24 h at −110 °C at a pressure of $6{\cdot}10^{-2}$ mbar. The freeze-dried products were placed in a desiccator for at least 4 h prior to handling. The final solutions of CVH-174, ritonavir, and zosuquidar when formulated as an amorphous formulation without HPMC-5 had concentrations of 9.4 mg/mL, 5.3 mg/mL, and 8.3 mg/mL, respectively. The solutions were transferred to individual falcon tubes (Sarstedt, DE) and placed in a −80 °C freezer for at least 3 h before freeze-drying. The same procedure for freezing the ASDs was applied to the amorphous controls. The ASDs were blended in an electric coffee mill (Køkkenchef, Skanderborg, DK) to obtain cloudy powders for the dissolution studies. Since the amorphous controls were brittle, a spatula was simply used to generate fine powders.

ASDs for the *in vivo* study were prepared as described above, where separate solutions of 8.0 mg/mL CVH-174, 4.4 mg/mL ritonavir, or 2.2 mg/mL zosuquidar, all with approximately 40 mg/mL HPMC-5 in 70 % (v/v) *tert*-butanol in ultra-pure water were placed in an –80 °C freezer for at least 3 h before freeze-drying in a Heto Drywinner freeze-dryer (Model DW 1,0–110, Alleroed, DK) for 24 h at –110 °C with a pressure of $6{\cdot}10^{-2}$ mbar. The freeze-dried products were placed in a desiccator for at least 4 h before being blended in an electric coffee mill (Køkkenchef, Skanderborg, DK) to obtain cloudy light-orange, white, and light-yellow powders of CVH-174, ritonavir, and zosuquidar, respectively.

All ASDs and amorphous controls for both the dissolution studies and *in vivo* study were stored at –18 °C and protected from light.

2.4.1. Solid-State Characterization with X-ray Powder diffraction

X-ray powder diffraction (XRPD) was carried out on a PANalytical X'PERT Pro (Malvern PANalytical Ltd, UK) with a Cu Kα source, at a voltage of 45 kV, and a current of 40 mA. Scanning was performed at a diffraction angle (2θ) from 5 to 90° with a run time of 10.01 min.

2.5. Dissolution studies

The principle of the presented dissolution study was performed and designed based on two dissolution studies performed by Nielsen et al. (2023) and Petersen et al. (2024). A modified dissolution-like setup was applied in a Talboys Professional Incubating Microplate Shaker (MERCK, Copenhagen, DK) with a temperature set at 37 °C and shaking at 160 rpm. Three beakers (100 mL, 50 × 70 mm) per dissolution study were used as dissolution vessels, covered with aluminum foil, and a USP type 1 basket was used as a sinker. Inside the basket, the separate amorphous solid dispersions (ASDs), crystalline or amorphous materials, were weighed and placed with the open end downwards on the bottom of the beaker. The dissolution studies were started by adding 80 mL pre-heated (37 °C) FaSSIF-V2, pH 6.50, to the beakers. Sampling was performed at 1, 5, 10, 15, 20, 30, and 45 min and 1, 2, 3, 4, 5, and 6 h by aspirating 0.50 mL media with a Henke-Ject 1 mL syringe (Henke Sass Wolf, Tuttlingen, DE) fitted with a Fine-Ject needle (Henke Sass Wolf, Tuttlingen, DE). The samples were immediately filtered through a 0.2 μm Minisart® filter (Regenerated Cellulose (RC 4), Sartorius Stedim, Stonehouse, UK), except for samples from the dissolution studies of the ASD with CVH-174, where the samples were first centrifuged in a microcentrifuge 157.MP (Ole Dich Instrument makers APS, Hvidovre, DK) with hard acceleration at 10,000 g at 30 °C for 5 min before filtering, to ensure the filter stayed intact due to high viscosity. The first 200 μL of the filtrate was discarded and the rest was collected. 150 μL of the collected sample was diluted 1:1 with 2 % (v/v) acetic acid in MeCN and analyzed by HPLC-UV as described above (Section 2.3).

Different setups were applied (Table 1) to investigate the dissolution of CVH-174, zosuquidar, and ritonavir as separate ASDs, amorphous materials, unprocessed CVH-174 2HCl, and ritonavir and zosuquidar 3HCl as crystalline materials. The dissolution profiles of unprocessed CVH-174 2HCl, crystalline ritonavir, and crystalline zosuquidar 3HCl were investigated individually in a dissolution vessel per compound. Whereas the dissolution profiles of the amorphous control of CVH-174 and ritonavir were investigated in the same dissolution vessel, the amorphous control of zosuquidar was investigated in a dissolution vessel alone since zosuquidar and CVH-174 could not be analysed together as both compounds absorb at 240 nm and 254 nm with the same retention time therefore it was not possible to separate the two compounds. The dissolution profiles of the separate ASDs containing CVH-174, ritonavir, or zosuquidar were investigated individually in a dissolution vessel. To investigate the ability to enhance the apparent solubility of CVH-174, the experiments were designed with doses corresponding to approximately 2.5-times the equilibrium solubility in FaSSIF-V2, pH 6.50 at 37°C, for all dissolution profiles. To investigate the ability to enhance the apparent solubility of ritonavir, the experiments were designed with

Table 1
Overview of *in vitro* dissolution setups, unprocessed or crystalline, amorphous, and applied amorphous solid dispersions of CVH-174 2HCl or CVH-174, ritonavir, and zosuquidar 3HCl or zosuquidar in vessels containing 80 mL FaSSIF-V2 pH 6.50 at 37 °C.

#	Applied setups	CVH-174 2HCl or CVH-174 added in dissolution vessel (mg)	Zosuquidar 3HCl or zosuquidar added in dissolution vessel (mg)	Ritonavir added in dissolution vessel (mg)	Times equilibrium solubility of CVH-174	Times equilibrium solubility of Zosuquidar	Times equilibrium solubility of Ritonavir
Drug release from unprocessed/crystalline materials, amorphous materials, or separate ASDs containing either CVH-174 2HCl or CVH-174, zosuquidar 3HCl or zosuquidar, or ritonavir.							
1	Unprocessed CVH-174 2HCl	26 ± 0.71			2.6 ± 0.071		
2	Crystalline Ritonavir			0.83 ± 0.088			3.14 ± 0.33
3	Crystalline Zosuquidar 3HCl		8.7 ± 0.18			1.5 ± 0.030	
4	Amorphous CVH-174 + Ritonavir	24 ± 0.42		2.3 ± 0.12	2.6 ± 0.045		8.7 ± 0.44
5	Amorphous Zosuquidar		7.5 ± 0.17			1.6 ± 0.036	
6	CVH-174 in HPMC-5	24 ± 0.59			2.6 ± 0.065		
7	Ritonavir in HPMC-5			0.27 ± 0.018 1.3 ± 0.037 2.7 ± 0.026			1.0 ± 0.066 5.0 ± 0.14 10 ± 0.099
8	Zosuquidar in HPMC-5		4.893 ± 0.009			1.009 ± 0.002	

doses corresponding to approximately the equilibrium solubility, and 5 and 10 times the equilibrium solubility in FaSSIF-V2, pH 6.50 at 37 °C. For the dissolution profile of crystalline ritonavir and the amorphous control of ritonavir, it was aimed to weigh out the equilibrium solubility, however, since the amount that should have been weighed was low (0.26 mg), the lowest possible ritonavir amount was weighed instead. Based on the previous study by Nielsen et al. (2023) it was known that zosuquidar formulated as an HPMC-5 ASD, and as an amorphous material, was not capable of enhancing the apparent solubility of zosuquidar. Therefore, it was chosen to design dissolution profiles with doses corresponding to approximately 1 to 1.5 times its equilibrium solubility in FaSSIF-V2, pH 6.50 at 37 °C.

2.6. *In vivo pharmacokinetic study of CVH-174 in Sprague-Dawley rats*

All animal procedures were approved by the Danish Animal Experiments Inspectorate under the Ministry of Food, Agriculture and Fisheries of Denmark (License no. 2024–15-0201–01641).

2.6.1. *Animals*

Twenty-four male Sprague Dawley rats (RjHan:SD, Janvier Labs, France) weighing 305.7 ± 11.7 g at the time of dosing, were randomly assigned to six groups of four rats and housed in individually ventilated cages (Allentown Rat 1800 cage), with each cage containing one group.

The rats were housed under controlled conditions with a temperature of 21 ± 1 °C, relative humidity of 45–65 %, and a 12-hour light/dark cycle with ad libitum access to food (Altromin 1324, Brogaarden, Lynge, Denmark) and water. Environmental enrichment consisted of Sizzlenest and cocoon nesting material, hemp rope, an aspen gnawing stick, an aspen ball, a red tunnel, and a red plastic house. Food enrichment included Bio Sev Pina Colada round pellets given every Monday, and Hazelnuts given every Thursday. The rats underwent a 14-day acclimatization period, during which they were trained and socialized. Training included habituation to the fixator in their home cage to minimize stress during the blood sampling procedures. The rats were also introduced to treats, including Mardi Gras Foraging Mix, Veggie-Bites, and glucose water, which were used both during the training sessions and as a post-procedure reward. Food and treats were deprived 17 h prior to dosing, and access was returned 1-hour post-dosing.

The rats were free of pathogens according to the FELASA recommendations (Mähler Convenor et al., 2014).

2.6.2. *Design of dosing and sampling*

Five groups were dosed per oral (PO) by gavage and received a dose of 27 ± 2.2 mg/kg CVH-174 as an HPMC-5-based ASD or 31 ± 0.24 mg/kg CVH-174 2HCl (28 ± 0.22 mg/kg CVH-174). One group was co-administrated with 10 ± 0.10 mg/kg ritonavir as an HPMC-5-based ASD, another group with 15 ± 1.9 mg/kg zosuquidar as an HPMC-5-based ASD, and one group was co-administrated with 10 ± 0.080 mg/kg ritonavir and 17 ± 0.14 mg/kg zosuquidar both as HPMC-5-based ASDs. The formulations were suspended in 10.00 mL FaSSIF-V2, pH 6.50 immediately prior to dosing, and administered as 5 mL/kg. When CVH-174 was co-administered with ritonavir and zosuquidar, two to three separate ASDs were physically mixed before suspension. One group was dosed intravenously (IV) with a single dose of 2.9 ± 0.030 mg/kg CVH-174 administered as 3.2 ± 0.030 mL/kg in ultra-pure water adjusted to pH 4.5 with NaOH and 295 mOsm/kg with glycerol. Before dosing, the IV solution was filtered through a 0.2 μm Whatman Puradisc, PTFE, sterile filter. The concentration of the IV solution was validated (by LC-MS/MS) and was visually inspected for particles before dosing, and no particles or change in color was observed. Dosing was performed between 08:00 and 11:00 AM. An overview of the administration description and how the formulations were combined is shown in Table 2.

Blood samples were collected from the lateral tail vein at intervals of 5, 10, 30, 45, 60, 120, 180, and 240 min after dosing, with the collection of approximately 100 μl blood per sample in Microvette® CB 300 K2E tubes (SARSTEDT AG & Co. KG, Nümbrecht, Germany). The rationale for this sampling schedule was based on the expected rapid absorption, high clearance, and half-life of CVH-174. Due to low amounts of blood collected from the rats who were giving the IV treatment, the first two datapoints in the pharmacokinetic profile in Fig. 6.**A** represent two measurements from two rats instead of three or four as the PO administrations.

Lidocaine gel (xylocaine 20 mg/g) was applied to the tail prior to blood sampling to minimize discomfort. After the last blood sample, the animals were euthanized using CO_2 in accordance with ethical guidelines. Plasma was obtained after centrifugation at 3,000 g for 10 min at 4 °C and stored at –18 °C until further bioanalysis.

2.6.3. *Sample preparation and bioanalysis*

The calibration standards were prepared by spiking rat plasma with a 10-times concentration of CVH-174 and mixed. The calibration standards for quantifying CVH-174 in the plasma samples ranged from 0.025 μg/mL to 2.5 μg/mL in the present studies. The calibration standards and plasma samples were precipitated by adding a 3-fold volume of 0.17 μg/mL Lefamulin Acetate (internal standard) in 80 % (v/v) MeCN in ultra-pure water containing 1 % (v/v) formic acid (FA). The samples were vortexed for 6 min and then centrifuged at 10,000 g and 22 °C for 10 min. Approximately 40 μL of the supernatant was transferred to HPLC vials and quantified using the LC-MS/MS method described below.

An injection volume of 5 μL was introduced into the LC-MS apparatus. The mobile phase consisted of 100 % (v/v) ultra-pure water containing 0.1 % (v/v) FA (A) and 100 % (v/v) MeCN containing 0.1 % (v/v) FA (B). A progressive change in the flow rate and the composition of mobile phase B was employed to facilitate separation (ranging from 10 % to 100 % B) within 6 min, followed by a return to 10 % B over the subsequent 2 min. The entire process was completed within 8 min. The flow rate began at 0.350 mL/min, gradually increasing to 0.750 mL/min over 6 min. In the ensuing 2 min, the flow rate was reverted to its initial conditions. The separation of the samples occurred on a reversed-phase LC column (Phenomenex XB-C18, 3 μm, 100 Å, 4.6x50mm, Phenomenex, Torrance, CA, USA) maintained at 50 °C. Once the analyte from the injection traversed the LC column, it underwent ionization through electrospray ionization (ESI) within an Agilent QQQ (6460 series) mass spectrometer. The instrument operated with a capillary voltage of 4 kV. The drying gas was heated to 250 °C with a flow rate of 13 L/min. Additionally, the gas temperature was set to 250 °C, accompanied by a flow rate of 80 L/h. The mass transition for CVH-174 of 724 → 421 *m/z*

Table 2
Overview of the administration description and the formulations used for the *in vivo* pharmacokinetic study.

Administration description and formulation/-s
IV: CVH-174
PO: CVH-174 2HCl
PO: CVH-174 in HPMC-5
PO: CVH-174 in HPMC-5 + ritonavir in HPMC-5
PO: CVH-174 in HPMC-5 + zosuquidar in HPMC-5
PO: CVH-174 in HPMC-5 + ritonavir in HPMC-5 + zosuquidar in HPMC-5

(CE22) was tracked, while for Lefamulin 508 → 201 *m/z* (CE26). For the acquisition of data, the Agilent Mass Hunter (B.08) software was employed, while the calculation of peak responses was performed using Agilent quantitative analysis (B.07).

2.7. Data analysis

The area under the curve from 0–4 h ($AUC_{0–4h}$) was calculated in GraphPad Prism 10.1.2 with the area under the curve analysis function. For the pharmacokinetic profiles without a visually clear elimination phase, the bioavailability was calculated using the $AUC_{0–4h}$ and the appropriate dose for the respective profile. The elimination phases were apparently evident for the pharmacokinetic profiles of CVH-174 co-administered with zosuquidar and CVH-174 co-administered with ritonavir and zosuquidar. The elimination rate constant (k_{el}) was calculated by linear regression of the linear part of the ln (plasma concentration) versus time profile (3–4 time points), where k_{el} was minus slope. The AUC from 0 to infinity (∞) was calculated:

$$AUC_{0-\infty} = AUC_{0-4h} + \left(\frac{C_{pt}}{k_{el}}\right) \quad (1)$$

where C_{pt} is the plasma concentration at the last quantifiable time point. The bioavailability of the pharmacokinetic profiles with an elimination was calculated using $AUC_{0-\infty}$ and the appropriate dose, whereas in the absence of a clear elimination phase only $AUC_{0–4h}$ is reported.

2.8. Statistics

The statistical analysis was done using GraphPad Prism 10.1.2, where n represents the number of replicates/animals. Unless otherwise

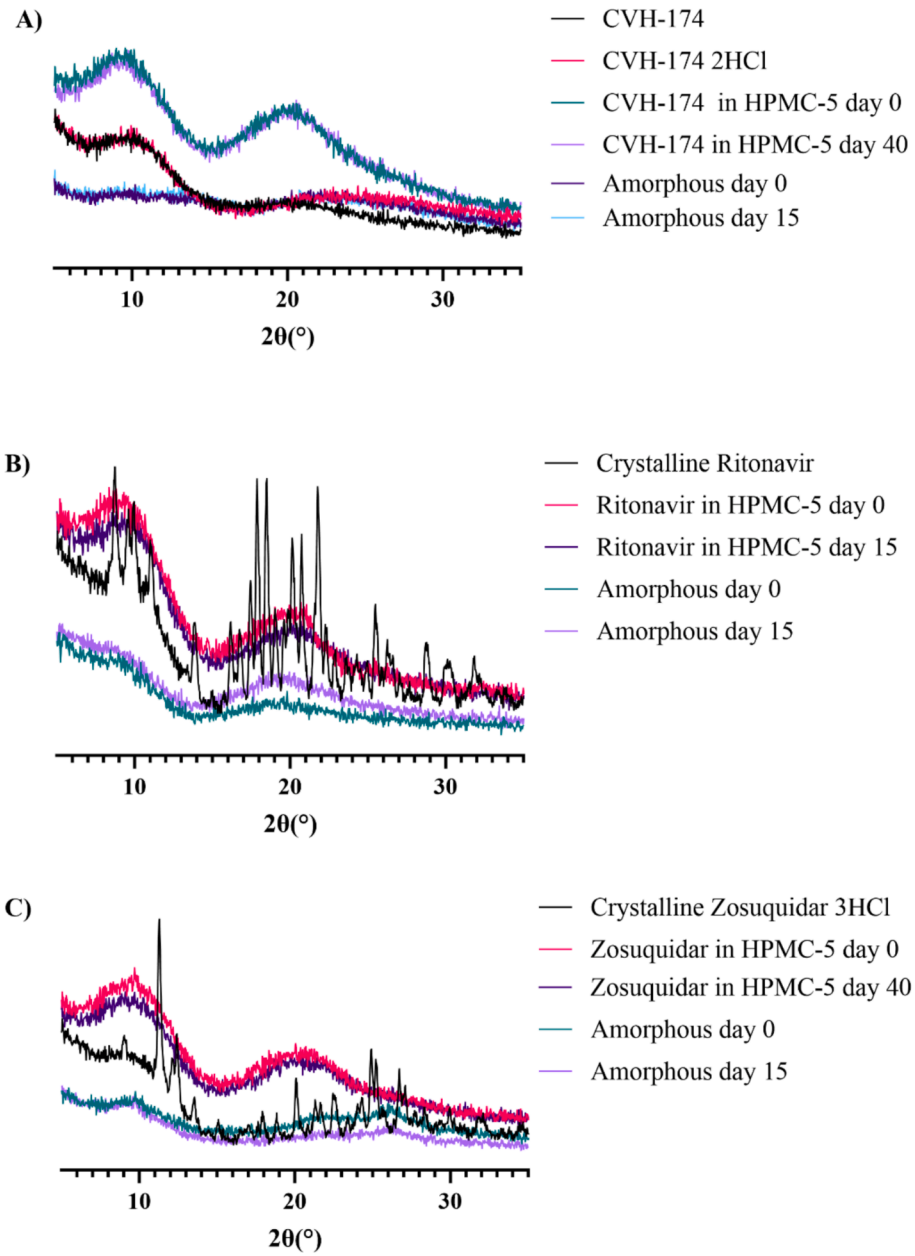

Fig. 1. X-ray Powder Diffractograms of CVH-174 **(A)**, ritonavir **(B)**, and zosuquidar **(C)** in HPMC-5-based ASDs, CVH-174, CVH-174 2HCl, crystalline ritonavir, crystalline zosuquidar 3HCl, and amorphous compounds of CVH-174, ritonavir, and zosuquidar when prepared for the dissolution studies. Moreover, 15 days (for amorphous controls) and 40 days (for ASDs) after preparation to investigate the formulations' stability and ensure that the formulations used in the dissolution studies had not re-crystallized during storage.

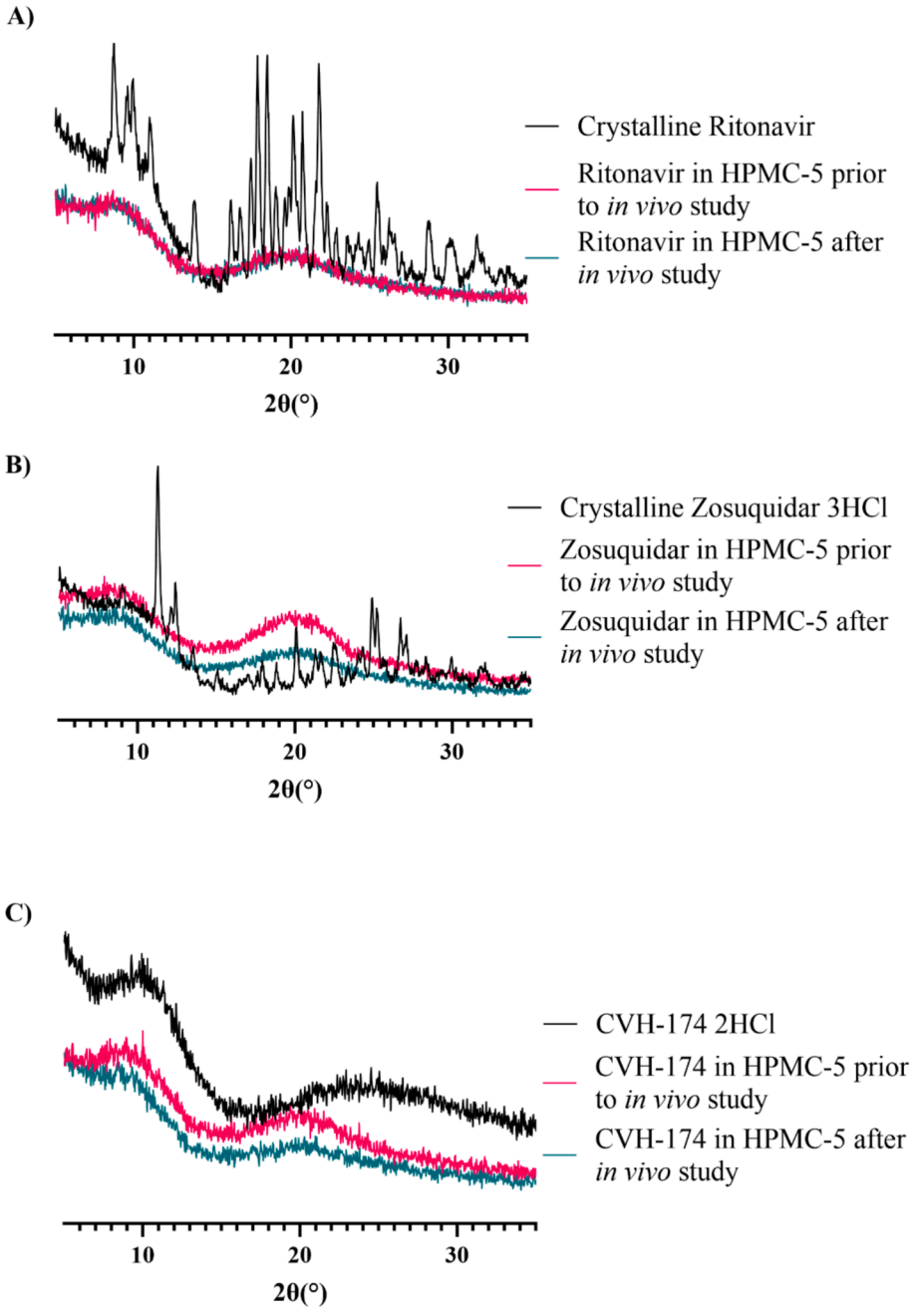

Fig. 2. X-ray Powder Diffractograms of ritonavir **(A)**, zosuquidar **(B)**, and CVH-174 **(C)** in HPMC-5-based ASDs, unprocessed CVH-174 2HCl, crystalline ritonavir, and crystalline zosuquidar 3HCl when prepared for the *in vivo* studies. Moreover, 4 days after the *in vivo* studies were performed. The re-investigation ensured that the formulations prepared for the *in vivo* studies had not re-crystallized.

stated, results are presented as mean values ± SEM (standard error of the mean).

3. Results

3.1. Solid state characterization of the ASDs

Ritonavir and zosuquidar 3HCl were used as received from the supplier and showed well-defined peaks in their X-ray Powder Diffraction (XRPD) diffractograms. Unprocessed CVH-174 2HCl showed clear halos without any peaks, as well as CVH-174 (Fig. 1). The diffractograms of the ASDs and amorphous controls showed clear halos without any peaks (Fig. 1).

The ASDs of CVH-174, ritonavir, and zosuquidar formulated for the *in vivo* study were re-investigated four days after the *in vivo* study and all diffractograms showed clear halos with no peaks (Fig. 2).

3.2. Apparent solubility enhancement of ritonavir by formulating an HPMC-5-based ASD

The equilibrium solubility of ritonavir in FaSSIF-V2, pH 6.50 at 37 °C was 4.6 ± 0.92 μM (3.3 ± 0.7 μg/mL). As shown in Fig. 3, the dissolution of crystalline ritonavir indicated that this equilibrium solubility was not reached during the 6-hour dissolution study and that the maximum concentration reached was 1.6 ± 0.30 μM, approximately 3-fold lower than the equilibrium solubility (Fig. 3). However, the dissolution of amorphous ritonavir did not seem to differentiate from the dissolution of crystalline ritonavir. The dissolution of amorphous ritonavir did not reach the equilibrium solubility and reached a maximum concentration of 1.3 ± 0.18 μM, approximately 3.5-fold lower than the equilibrium solubility, similar to crystalline ritonavir.

The ability to enhance the apparent solubility of ritonavir after dissolution from an HPMC-5-based ASD at different doses corresponding to 1-times, 5-times, and 10-times the equilibrium solubility in FaSSIF-V2, pH 6.50, was also investigated. At a dose of ritonavir in the dissolution vessel corresponding to the equilibrium solubility, the equilibrium solubility was reached after 20 min with a concentration of 4.5 ± 0.40 μM, being approximately 3- and 3.5-fold higher than the maximal concentration reached for crystalline and amorphous ritonavir, respectively. HPMC-5 enhanced the apparent solubility of ritonavir to approximately 23 ± 1.3 μM and 54 ± 7.1 μM, corresponding to approximately 5- and 10-times the equilibrium solubility of ritonavir,

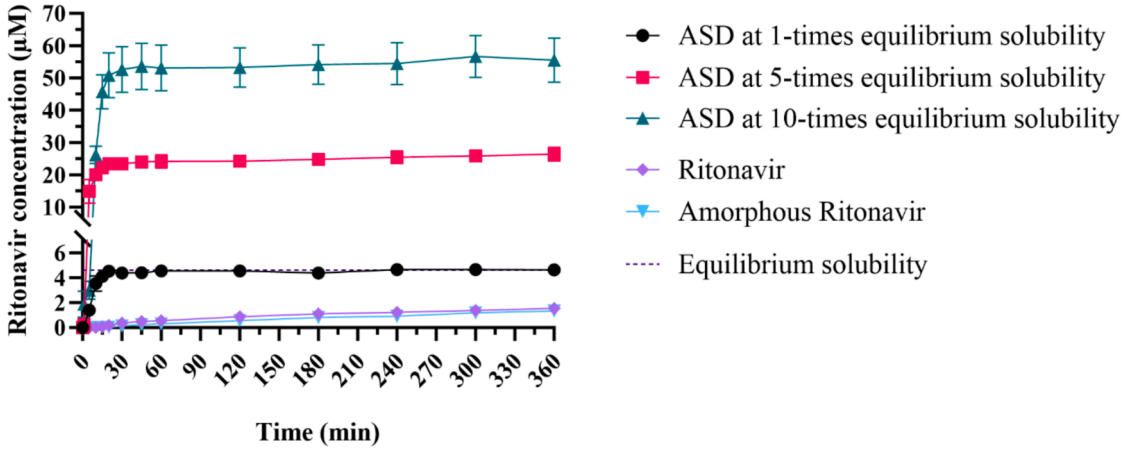

Fig. 3. Dissolution profiles of an HPMC-5-based amorphous solid dispersion (ASD) with ritonavir at doses corresponding to approximately 1-, 5-, and 10-times the equilibrium solubility in 80 mL FaSSIF-V2 pH 6.50 at 37 °C. Dissolution profiles of crystalline ritonavir at a dose corresponding to approximately 3-times the equilibrium solubility, and amorphous ritonavir at a dose corresponding to approximately 9-times the equilibrium solubility in 80 mL FaSSIF-V2 pH 6.50 at 37 °C. The concentration (μM) of ritonavir is plotted as a function of the sampling time point in minutes (min). Data points for the ASDs and crystalline material are reported as mean values (mean ± SEM, n = 3). SEMs smaller than the symbol size are not shown. Data points for amorphous material are reported as mean values (n = 2).

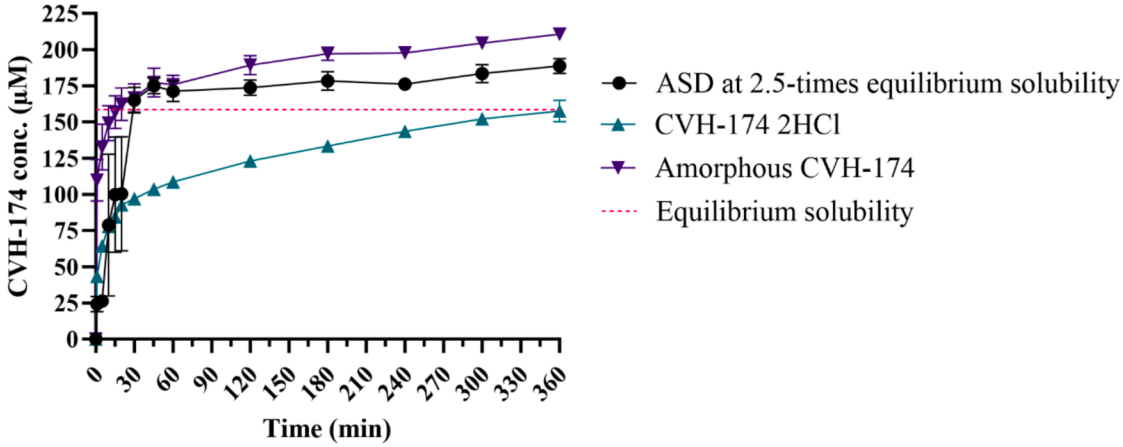

Fig. 4. Dissolution profiles of an HPMC-5-based amorphous solid dispersion (ASD) with CVH-174, unprocessed CVH-174 2HCl, and an amorphous control of CVH-174 at doses corresponding to approximately 2.5-times the equilibrium solubility in 80 mL FaSSIF-V2 pH 6.50 at 37 °C. The concentration (μM) of CVH-174 is plotted as a function of the sampling time point in minutes (min). Data points are reported as mean values (mean ± SEM, n = 3). SEMs smaller than the symbol size are not shown.

respectively. The dissolution profiles of ritonavir at the two different doses corresponding with 5- and 10-times the equilibrium solubility indicated that they differed from each other and the dissolution profile of the dose corresponding with 1-time the equilibrium solubility when comparing the dissolution time before reaching equilibrium solubility. The dissolution time needed to reach equilibrium solubility increased, thereby making the dissolution slower, by 10 min when adding ritonavir at a dose corresponding to 5-times the equilibrium solubility and a further 15 min increase was observed when adding a dose corresponding to 10-times the equilibrium solubility. These results indicate a slower dissolution of ritonavir from the HPMC-5-based ASD when a larger amount of ritonavir and HPMC-5 is present in the dissolution setup.

3.3. Dissolution from HPMC-5-based ASDs of CVH-174 and zosuquidar

The equilibrium solubility of CVH-174 in FaSSIF-V2, pH 6.50 at 37 °C was 158.41 ± 1.01 μM (120 ± 0.73 μg/mL). The dissolution of unprocessed CVH-174 2HCl reached the equilibrium solubility after 6 h of the dissolution study (Fig. 4). In contrast, the dissolution profile of amorphous CVH-174 reached the equilibrium solubility at approximately 15 min, having the fastest dissolution rate. Within 45 min, 177 ± 10 μM of CVH-174 was reached, which increased to 211 ± 1.5 μM during the 6-hour dissolution study. The concentration did however not reach 2.5-times of the equilibrium solubility. Furthermore, the dissolution profiles in Fig. 4 show that during the 6-hour dissolution study, amorphous CVH-174 reached a higher concentration than the unprocessed CVH-174 2HCl. To investigate if it is possible to enhance the apparent solubility of CVH-174, an HPMC-5-based ASD was prepared. A dissolution study at a dose corresponding to 2.5-times the equilibrium solubility of CVH-174 in FaSSIF-V2, pH 6.50 at 37 °C, was performed and compared to the dissolution profile of unprocessed CVH-174 2HCl and amorphous CVH-174. The dissolution profile of CVH-174 in the HPMC-5-based ASD reached the equilibrium solubility at approximately 30 min. The dissolution profile did not indicate that a plateau was reached, as a concentration of 174.99 ± 5.42 μM was reached after 45 min which increased slowly to 188.66 ± 5.20 μM during the 6-hour dissolution study. However, once again the concentration was unable to reach 2.5-times equilibrium solubility during the 6-hour dissolution study. As the amorphous CVH-174 reached the equilibrium solubility 15 min before the HPMC-5-based ASD, this indicates a faster dissolution rate of CVH-174 when HPMC-5 is absent and faster dissolution than unprocessed CVH-174 2HCl.

The equilibrium solubility of zosuquidar in FaSSIF-V2, pH 6.50 at 37 °C was 114.96 ± 1.81 μM (61.0 ± 0.95 μg/mL). The dissolution profile of crystalline zosuquidar 3HCl indicates that a concentration of 64.40 ± 0.22 μM zosuquidar was reached after 20 min and thereafter slowly increased to 79.40 ± 1.89 μM corresponding to 69 % of its determined equilibrium solubility (Fig. 5). The dissolution profile of zosuquidar from amorphous material was similar to the dissolution profile of crystalline zosuquidar 3HCl (Fig. 5). However, a 1.3-fold concentration increase was observed after 20 min when compared to the crystalline zosuquidar 3HCl which slowly increased to 107.14 ± 2.34 μM, corresponding to 93 % of the determined equilibrium solubility. The dissolution of the HPMC-5-based ASD containing zosuquidar reached a plateau after 60 min, with a mean concentration of 98.55 ± 1.00 μM, being 85 % of the determined equilibrium solubility (Fig. 5). The dissolution profiles of zosuquidar in the different formulations indicate that it was not possible to reach the equilibrium solubility determined. Nevertheless, it was possible to facilitate apparent solubility enhancement.

3.4. Bioavailability of CVH-174 after co-administration with zosuquidar and ritonavir in polymer-based ASDs

The pharmacokinetic profile of CVH-174 was first evaluated after intravenous (IV) administration to Sprague Dawley rats, where the plasma concentration decreased rapidly (Fig. 6.**A**). The data was fitted to a one-compartment model with an initial maximal plasma concentration of 20.7 μg/mL, an $AUC_{0-\infty}$ of 4.1 ± 1.1 μg/mL × h, an elimination rate constant of 4.5 h^{-1} (95 % CI of 3.4 – 6.0 h^{-1}) resulting in a half-life of 0.15 h (95 % CI of 0.12 – 6.0). The oral (PO) administration of CVH-174 as unprocessed compound (i.e., amorphous from the synthesis and purification) and formulated as an HPMC-5-based ASD (Fig. 6.**B**) showed similar kinetic profiles with low plasma concentrations and without a clear definition of an absorption process with no clear maximal plasma concentrations, and AUC_{0-4h}s of 0.38 ± 0.043 μg/mL × h and 0.54 ± 0.11 μg/mL × h, respectively. Oral administration of CVH-174 formulated as an HPMC-5-based ASD with the P-gp inhibitor zosuquidar (Fig. 6.**C**) did not cause any effect on the plasma concentrations or the pharmacokinetic profile as the $AUC_{0-\infty}$ was 0.80 ± 0.37 μg/mL × h and the bioavailability was 2.4 ± 1.1 %. However, formulating CVH-174 in an HPMC-5-based ASD with the CYP3A4 inhibitor ritonavir resulted in a different kinetic profile with a maximal plasma concentration (C_{max}) of around 0.5 μg/mL at approximately 0.17 h. The AUC_{0-4h} was 1.4 ± 0.088 μg/mL × h, resulting in a significant increase in AUC being almost 350 % higher than the administration of the unprocessed CVH-174 2HCl alone. After administration with both zosuquidar and ritonavir, the AUC_{0-4h} increased further to 7.1 ± 2.0 μg/mL × h with a C_{max} of around 0.7 μg/mL at approximately 2 h. The absolute bioavailability increased to 18.4 ± 5.3 %, resulting in a significant increase in bioavailability

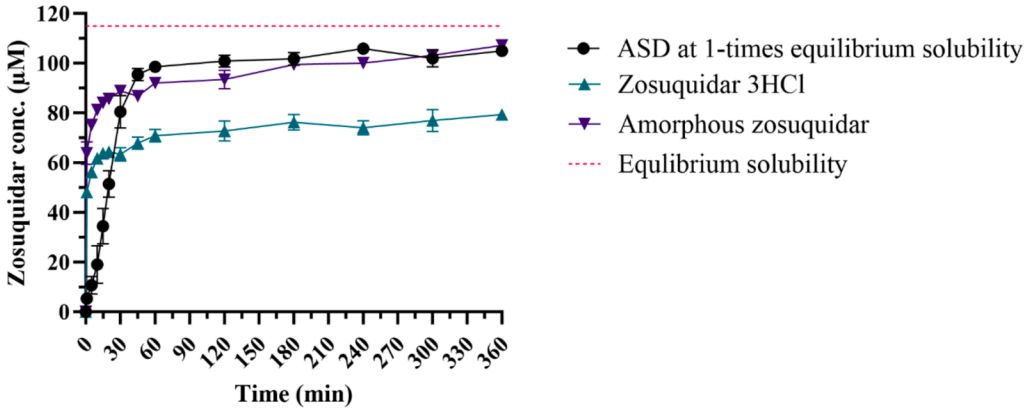

Fig. 5. Dissolution profiles of an HPMC-5-based amorphous solid dispersion (ASD) with zosuquidar, crystalline zosuquidar 3HCl, and the amorphous control of zosuquidar at doses corresponding to approximately 1-, 1.5-, and 1.5-times the equilibrium solubility in 80 mL FaSSIF-V2 pH 6.50 at 37 °C, respectively. The concentration (μM) of zosuquidar is plotted as a function of the sampling time point in minutes (min). Data points are reported as mean values (mean ± SEM, n = 3). SEMs smaller than the symbol size are not shown.

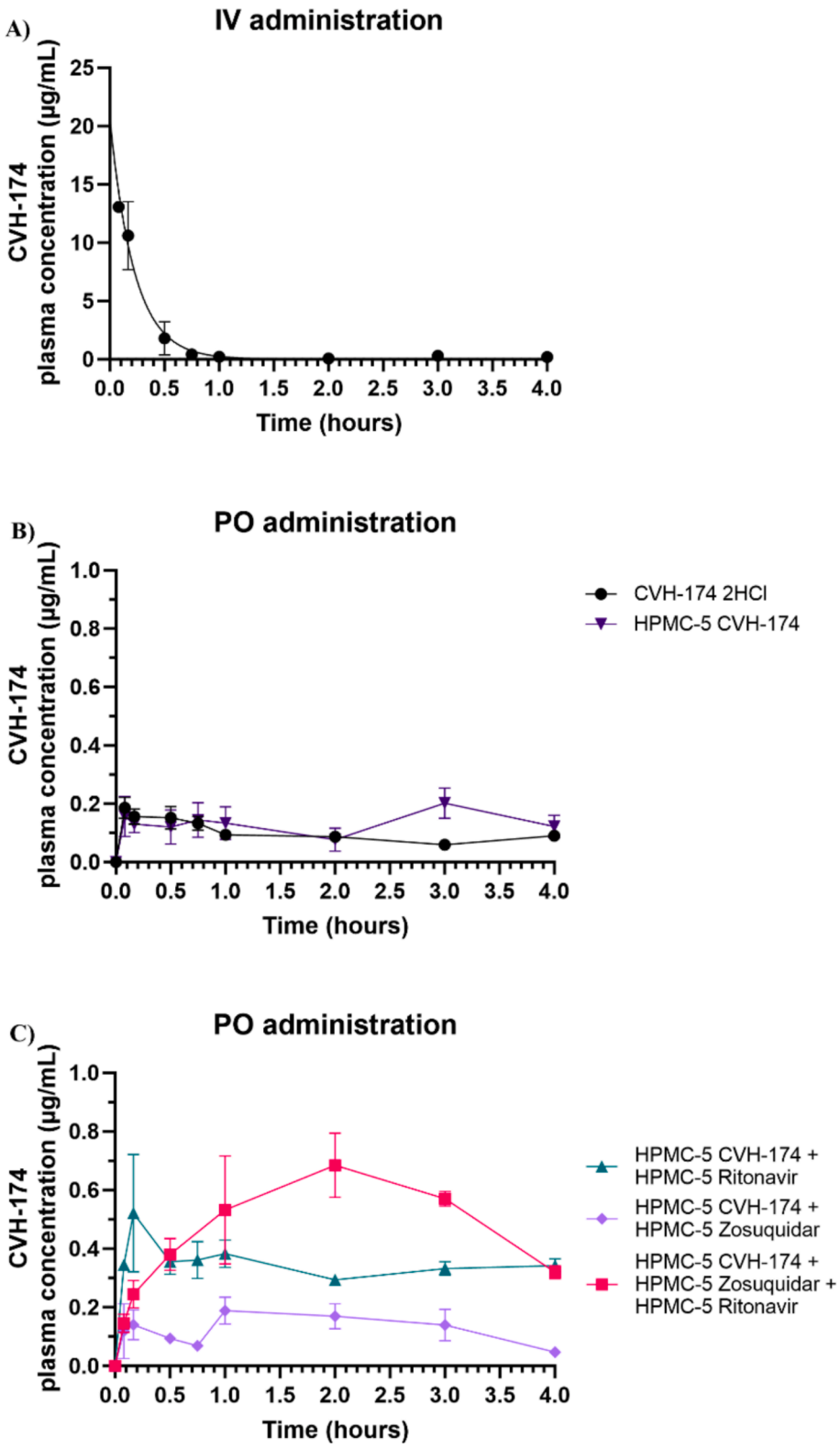

Fig. 6. Pharmacokinetic profiles of CVH-174 after intravenous (IV) and per oral (PO) administration to fasted male Sprague Dawley rats. (A) Pharmacokinetic profiles after IV administration of 2.9 ± 0.030 mg/kg CVH-174 administered in ultra-pure water and glycerol. The first two data points on the profile are shown as mean, n = 2, whereas the rest are shown as mean ± SEM, n = 3–4. SEMs smaller than symbol size are not shown. (B) Pharmacokinetic profiles after PO administration of 28 mg/kg CVH-174 administered as unprocessed CVH-174 2HCl, and 27 mg/kg CVH-174 as an amorphous solid dispersion (ASD) in HPMC-5. (C) Pharmacokinetic profiles after PO administration of 27 mg/kg CVH-174 as an HPMC-5-based ASD co-administered with 10 mg/kg ritonavir as an HPMC-5-based ASD, CVH-174 co-administered with 15 mg/kg zosuquidar as HPMC-5-based ASDs, and CVH-174 co-administered with 10 mg/kg ritonavir and 17 mg/kg zosuquidar as HPMC-5-based ASDs. Straight connecting lines for illustrative purposes. Data are shown as mean ± SEM, n = 3–4. SEMs smaller than symbol size are not shown.

being almost 18-fold higher than the administration of the unprocessed CVH-174 2HCl alone.

4. Discussion

There is a need for new antibiotic drug substances to fight the increasing number of multi-drug-resistant bacteria (World Health Organization, 2024). One class of potential new antibiotics is pleuromutilins, which are attractive due to their low rate of resistance development and high activity (Eyal et al., 2016; Eyal et al., 2015; Goethe et al., 2019; Högenauer and Ruf, 1981). They are on the other hand challenged by enzymatic lability, recognition by P-gp, and in some cases low solubility (Goethe et al., 2019; Heidtmann et al., 2024; Zeitlinger et al., 2016). Recently, we suggested CVH-174 as a new potential pleuromutilin drug candidate, however, the compound was a high-affinity substrate of CYP3A4, a weak substrate of P-gp, and had a poor solubility, resulting in almost no oral bioavailability in mice and pigs (Heidtmann et al., 2024). In the present publication, a formulation approach was used to increase the oral bioavailability of CVH-174 in rats, aiming to address the three factors a) solubility, b) first-pass/hepatic metabolism, and c) P-gp interaction. These are the most crucial factors *in vivo* for the future optimization of pleuromutilin drug candidates, whether through pharmaceutical formulation or a medicinal chemistry approach to develop new improved pleuromutilin drug candidates.

To increase the oral absorption of CVH-174 we used amorphous solid dispersions (ASDs) based on the HPMC-5 polymer. ASDs have traditionally been used to increase the solubility and bioavailability of poorly soluble drug substances (Fotaki et al., 2014; Kong et al., 2023; Li and Taylor, 2018). However, they have recently also been used to include transporter inhibitors such as P-gp inhibitors to increase drug substance absorption (Moes et al., 2013; Nielsen et al., 2023; Petersen et al., 2024), and to include enzyme inhibitors such as CYP3A4 inhibitors to decrease first-pass intestinal and hepatic metabolism of drug substances (Eagling et al., 1997; Hendrikx et al., 2014; Oostendorp et al., 2009; Sevrioukova and Poulos, 2010; Tomaru et al., 2013). Zosuquidar was selected as the inhibitor for P–gp due to its ability to increase the absorption of the P-gp substrate etoposide in the chosen preclinical *in vivo* model (Nielsen et al., 2021; Nielsen et al., 2023). The CYP3A4 inhibitor ritonavir was selected based on previous studies showing its potential to improve the absorption of another anti-HIV compound saquinavir (Kempf et al., 1997; Tomaru et al., 2013), and anti-cancer compounds such as paclitaxel, docetaxel, and cabazitaxel in rats and mice after co-administration of ritonavir (Hendrikx et al., 2014; Loos et al., 2023; Moes et al., 2013; Oostendorp et al., 2009). An important element of ASDs is the ability to control dissolution and induce a local supersaturation of the drug substance and/or inhibitor (Nielsen et al., 2023; Petersen et al., 2024). In the present study, the synthetic approach generated an amorphous salt of CVH-174, which was confirmed by XRPD and in accordance with what Heidtmann et al. (2024) reported. The salt could not be supersaturated using HPMC-5, likewise, the chosen P-gp inhibitor, zosuquidar, could not be supersaturated which is similar to what we have observed previously, although the solubility determined in the present study was approximately 1.5-fold higher than previously determined (Nielsen et al., 2023). In contrast, the dissolution of ritonavir from HPMC-5-based ASDs resulted in concentrations highly exceeding the measured equilibrium solubility in FaSSIF-V2 at pH 6.50 at 37 °C, thus suggesting that ritonavir can be supersaturated. Amorphous ritonavir could not be supersaturated, and the dissolution profile showed a relatively slow dissolution rate, compared to the HPMC-5-based ASD. Moreover, amorphous ritonavir did not differentiate from the dissolution profile of crystalline ritonavir. These observations could be explained by a) the rapid crystallization of amorphous ritonavir upon contact with FaSSIF-V2, and/or b) the ability of HPMC-5 to increase the surface area of ritonavir by decreasing the particle size and/or optimizing the wetting ability of ritonavir, cf. Noyes-Whitney equation (Leuner and Dressman, 2000). Future studies could therefore investigate the specific explanation of the poor dissolution rate and profile of amorphous ritonavir. Likewise, the stability of the ASD formulations is a critical factor to monitor to ensure that the compounds do not undergo rapid crystallization during storage. Here the formulations remained stable during the experiments, similar to what was previously observed for similar formulations (Nielsen et al., 2023; Petersen et al., 2024).

In terms of increasing the oral bioavailability of CVH-174, the results suggest that solubility is not the main reason for the limited bioavailability of CVH-174. CVH-174 is amorphous after synthesis and freeze-drying without HPMC-5 and with HPMC-5 formulated as an ASD to prevent precipitation. However, neither of the three formulation approaches affects the bioavailability, although the freeze-drying process influences the dissolution profile and the time to reach 50 % dissolution. It is possible that HPMC-5 is not the right spring /parachute for the compounds, and future studies could investigate if other polymers could induce a supersaturated state after dissolution. In contrast, the oral bioavailability significantly increased 3.5 times after the inclusion of ritonavir in the HPMC-5-based formulation. This points to a major role of CYP3A4 in limiting the oral bioavailability of CVH-174. In the present study, only a single dose of ritonavir was investigated, and therefore it is possible that we have not obtained the maximal increase in bioavailability possible. The dose of ritonavir given to the rats was approximately 3 mg, whereas the usual ritonavir dose for humans is 100 to 200 mg once or twice daily (Norvir®) or 100 mg up to twice daily (Kaletra®) (Laboratories, 2001; Morris et al., 2019; Vogel and Rockstroh, 2005). Moreover, in the present study, ritonavir was dosed simultaneously with CVH-174, however, it is possible that administering ritonavir a certain time before the CVH-174 may optimize the distribution of ritonavir and thereby maximize the inhibition of CYP enzymes. When the P-gp inhibitor zosuquidar was administered together with CVH-174 in HPMC-5-based ASDs no increase in bioavailability was observed. However, when zosuquidar and ritonavir were administered together with CVH-174, all formulated as HPMC-5-based ASDs, a large increase in the oral bioavailability and a different pharmacokinetic profile was observed, with a prolonged absorption phase and increased C_{max} and t_{max} compared to when ritonavir was the only inhibitor administrated. The prolonged absorption phase and elimination phase observed for CVH-174 when combined with ritonavir has been seen before for lopinavir, an HIV-1 protease inhibitor, when it was co-administered with ritonavir in male Sprague-Dawley rats (Sham et al., 1998). A number of events could explain the different pharmacokinetic profile; a) Zosuquidar inhibits the P-gp mediated efflux of ritonavir, which is also a P-gp substrate (Law et al., 2004; Lee et al., 1998; Loos et al., 2024; Sankatsing et al., 2004) and thus increases the cellular exposure to ritonavir leading to increased CYP3A4 inhibition. This suggests that CYP-mediated metabolism is the main limiting factor for CVH-174 bioavailability. b) As ritonavir inhibits the metabolism of CVH-174, the impact of P-gp, of which CVH-174 is a weak substrate, becomes important for membrane permeability, and hence zosuquidar increases oral bioavailability of CVH-174 under these conditions. Collectively, the present study used a formulation approach with transporter and enzyme inhibitors to increase the oral availability of a pleuromutilin drug candidate and opened for research to provide a further increase in bioavailability through future optimization.

5. Conclusion

The present study investigated whether CYP-mediated metabolism or P-gp recognition were the main limitations to developing oral formulations of CVH-174 and whether the oral bioavailability could be increased. The oral bioavailability of CVH-174 in Sprague-Dawley rats was surprisingly increased to approximately 18 % by the combined co-administration of ritonavir- and zosuquidar-containing ASDs. In conclusion, the oral bioavailability of CVH-174 can be significantly increased through a formulation design encompassing an inhibitor of the

CYP3A4 enzyme, which holds great potential for the future development of an inherent metabolic labile pleuromutilin drug class.

CRediT authorship contribution statement

Emilie Fynbo Petersen: Writing – review & editing, Writing – original draft, Investigation, Formal analysis, Data curation, Conceptualization. **Charlotte Laurfelt Munch Rasmussen:** Writing – review & editing, Writing – original draft, Supervision, Methodology, Investigation, Data curation, Conceptualization. **Bala Krishna Prabhala:** Writing – review & editing, Writing – original draft, Methodology, Investigation, Formal analysis, Data curation, Conceptualization. **Christoffer Vogsen Heidtmann:** Writing – review & editing, Writing – original draft, Resources, Funding acquisition, Conceptualization. **Poul Nielsen:** Writing – review & editing, Supervision, Resources, Project administration, Investigation, Funding acquisition. **Carsten Uhd Nielsen:** Writing – review & editing, Writing – original draft, Supervision, Resources, Project administration, Methodology, Investigation, Funding acquisition, Formal analysis, Conceptualization.

Funding

Innovation Fund Denmark (InnoExplorer grants 3140-00022B and 1047-00007), The Novo Nordisk Foundation (Pioneer Innovator, grant NNF21OC0072708) as well as Hørslevfonden are acknowledged for funding the project.

Declaration of competing interest

The authors declare the following financial interests/personal relationships which may be considered as potential competing interests: Poul Nielsen and Christoffer Heidtmann have patent #Antibacterial and antifungal pleuromutilin conjugates (WO2021219813) pending to CA US CN AU EP. Other authorsdeclare no competing financial interests or personal relationships that could have appeared to influence the work reported in this paper.

Acknowledgments

Louise Johansson is greatly acknowledged for helping with the equipment for freeze-drying all amorphous solid dispersions and amorphous controls, and Christian Ding Fisker for synthesizing compound CVH-174 2HCl for the study. Furthermore, the animal technicians Liv Holm and Anne-Mette Durand and animal technician trainee Signe Kroer Rimmen from the Biomedical Laboratory, University of Southern Denmark, are greatly acknowledged for their technical assistance during the *in vivo* study.

Data availability

Data will be made available on request.

References

Adhikary, S., Duggal, M.K., Nagendran, S., Chintamaneni, M., Tuli, H.S., Kaur, G., 2022. Lefamulin: a New Hope in the Field of Community-Acquired Bacterial Pneumonia. Curr. Pharmacol. Rep. 8, 418–426.

Eagling, V.A., Back, D.J., Barry, M.G., 1997. Differential inhibition of cytochrome P450 isoforms by the protease inhibitors, ritonavir, saquinavir and indinavir. Br. J. Clin. Pharmacol. 44, 190–194.

Eyal, Z., Matzov, D., Krupkin, M., Paukner, S., Riedl, R., Rozenberg, H., Zimmerman, E., Bashan, A., Yonath, A., 2016. A novel pleuromutilin antibacterial compound, its binding mode and selectivity mechanism. Sci. Rep. 6, 39004.

Eyal, Z., Matzov, D., Krupkin, M., Wekselman, I., Paukner, S., Zimmerman, E., Rozenberg, H., Bashan, A., Yonath, A., 2015. Structural insights into species-specific features of the ribosome from the pathogen Staphylococcus aureus. Proc. Natl. Acad. Sci. 112, E5805–E5814.

Falcó, V., Burgos, J., Almirante, B., 2020. An overview of lefamulin for the treatment of community acquired bacterial pneumonia. Expert Opin. Pharmacother. 21, 629–636.

Fong, I.W., 2023. Pleuromutilin: A New Class of Antibiotic: Lefamulin. In: Fong, I.W. (Ed.), New Antimicrobials: for the Present and the Future. Springer International Publishing, Cham, pp. 109–114.

Fotaki, N., Long, C.M., Tang, K., Chokshi, H., 2014. Dissolution of Amorphous Solid Dispersions: Theory and Practice. In: Shah, N., Sandhu, H., Choi, D.S., Chokshi, H., Malick, A.W. (Eds.), Amorphous Solid Dispersions: Theory and Practice. Springer, New York, New York, NY, pp. 487–514.

Goethe, O., Heuer, A., Ma, X., Wang, Z., Herzon, S.B., 2019. Antibacterial properties and clinical potential of pleuromutilins. Nat. Prod. Rep. 36, 220–247.

Hammond, J., Leister-Tebbe, H., Gardner, A., Abreu, P., Bao, W., Wisemandle, W., Baniecki, M., Hendrick, V.M., Damle, B., Simón-Campos, A., Pypstra, R., Rusnak, J. M., 2022. Oral Nirmatrelvir for High-Risk, Nonhospitalized Adults with Covid-19. N. Engl. J. Med. 386, 1397–1408.

Heidtmann, C.V., Fejer, A.R., Stærk, K., Pedersen, M., Asmussen, M.G., Hertz, F.B., Prabhala, B.K., Frimodt-Møller, N., Klitgaard, J.K., Andersen, T.E., Nielsen, C.U., Nielsen, P., 2024. Hit-to-Lead Identification and Validation of a Triaromatic Pleuromutilin Antibiotic Candidate. J. Med. Chem. 67, 3692–3710.

Hendrikx, J.J.M.A., Lagas, J.S., Rosing, H., Schellens, J.H.M., Beijnen, J.H., Schinkel, A. H., 2013. P-glycoprotein and cytochrome P450 3A act together in restricting the oral bioavailability of paclitaxel. Int. J. Cancer 132, 2439–2447.

Hendrikx, J.J.M.A., Lagas, J.S., Wagenaar, E., Rosing, H., Schellens, J.H.M., Beijnen, J. H., Schinkel, A.H., 2014. Oral co-administration of elacridar and ritonavir enhances plasma levels of oral paclitaxel and docetaxel without affecting relative brain accumulation. Br. J. Cancer 110, 2669–2676.

Högenauer, G., 1975. The mode of action of pleuromutilin derivatives. Location and properties of the pleuromutilin binding site on Escherichia coli ribosomes. Eur. J. Biochem. 52, 93–98.

Högenauer, G., Ruf, C., 1981. Ribosomal binding region for the antibiotic tiamulin: stoichiometry, subunit location, and affinity for various analogs. Antimicrob. Agents Chemother. 19, 260–265.

Hörter, D., Dressman, J.B., 2001. Influence of physicochemical properties on dissolution of drugs in the gastrointestinal tract1PII of original article: S0169-409X(96)00487-5. The article was originally published in Advanced Drug Delivery Reviews 25 (1997) 3–14.1. Adv. Drug Deliv. Rev. 46, 75–87.

Kavanagh, F., Hervey, A., Robbins, W.J., 1951. Antibiotic Substances From Basidiomycetes. Proc. Natl. Acad. Sci. 37, 570–574.

Kavanagh, F., Hervey, A., Robbins, W.J., 1952. Antibiotic Substances from Basidiomycetes. Proc. Natl. Acad. Sci. 38, 555–560.

Kempf, D.J., Marsh, K.C., Kumar, G., Rodrigues, A.D., Denissen, J.F., McDonald, E., Kukulka, M.J., Hsu, A., Granneman, G.R., Baroldi, P.A., Sun, E., Pizzuti, D., Plattner, J.J., Norbeck, D.W., Leonard, J.M., 1997. Pharmacokinetic enhancement of inhibitors of the human immunodeficiency virus protease by coadministration with ritonavir. Antimicrob. Agents Chemother. 41, 654–660.

Kong, Y., Wang, W., Wang, C., Li, L., Peng, D., Tian, B., 2023. Supersaturation and phase behavior during dissolution of amorphous solid dispersions. Int. J. Pharm. 631, 122524.

Laboratories., A., 2001. Norvir (ritonavir) package insert. Abbott Laboratories North Chicago, IL, USA.

Law, D., Schmitt, E.A., Marsh, K.C., Everitt, E.A., Wang, W., Fort, J.J., Krill, S.L., Qiu, Y., 2004. Ritonavir-PEG 8000 amorphous solid dispersions: in vitro and in vivo evaluations. J. Pharm. Sci. 93, 563–570.

Lee, C.G.L., Gottesman, M.M., Cardarelli, C.O., Ramachandra, M., Jeang, K.-T., Ambudkar, S.V., Pastan, I., Dey, S., 1998. HIV-1 Protease Inhibitors Are Substrates for the MDR1 Multidrug Transporter. Biochemistry 37, 3594–3601.

Lennard, P.R., Hiemstra, P.S., Nibbering, P.H., 2023. Complementary Activities of Host Defence Peptides and Antibiotics in Combating Antimicrobial Resistant Bacteria. Antibiotics (basel, Switzerland) 12, 1518.

Leuner, C., Dressman, J., 2000. Improving drug solubility for oral delivery using solid dispersions. Eur. J. Pharm. Biopharm. 50, 47–60.

Li, N., Taylor, L.S., 2018. Tailoring supersaturation from amorphous solid dispersions. J. Control. Release 279, 114–125.

Long, K.S., Hansen, L.H., Jakobsen, L., Vester, B., 2006. Interaction of pleuromutilin derivatives with the ribosomal peptidyl transferase center. Antimicrob Agents Chemother 50, 1458–1462.

Loos, N.H.C., Martins, M.L.F., de Jong, D., Lebre, M.C., Tibben, M., Beijnen, J.H., Schinkel, A.H., 2023. Enhancement of the Oral Availability of Cabazitaxel Using the Cytochrome P450 3A (CYP3A) Inhibitor Ritonavir in Mice. Mol. Pharm. 20, 2477–2489.

Loos, N.H.C., Martins, M.L.F., de Jong, D., Lebre, M.C., Tibben, M., Beijnen, J.H., Schinkel, A.H., 2024. Coadministration of ABCB1/P-glycoprotein inhibitor elacridar improves tissue distribution of ritonavir-boosted oral cabazitaxel in mice. Int. J. Pharm. 650, 123708.

Moes, J., Koolen, S., Huitema, A., Schellens, J., Beijnen, J., Nuijen, B., 2013. Development of an oral solid dispersion formulation for use in low-dose metronomic chemotherapy of paclitaxel. Eur. J. Pharm. Biopharm. 83, 87–94.

Morris, J.B., Tisi, D.A., Tan, D.C.T., Worthington, J.H., 2019. Development and Palatability Assessment of Norvir® (Ritonavir) 100 mg Powder for Pediatric Population. Int J Mol Sci. 2019 Apr 6;20(7):1718.

Murray, C.J.L., Ikuta, K.S., Sharara, F., Swetschinski, L., Robles Aguilar, G., Gray, A., Han, C., Bisignano, C., Rao, P., Wool, E., Johnson, S.C., Browne, A.J., Chipeta, M.G., Fell, F., Hackett, S., Haines-Woodhouse, G., Kashef Hamadani, B.H., Kumaran, E.A. P., McManigal, B., Achalapong, S., Agarwal, R., Akech, S., Albertson, S., Amuasi, J., Andrews, J., Aravkin, A., Ashley, E., Babin, F.-X., Bailey, F., Baker, S., Basnyat, B.,

Bekker, A., Bender, R., Berkley, J.A., Bethou, A., Bielicki, J., Boonkasidecha, S., Bukosia, J., Carvalheiro, C., Castañeda-Orjuela, C., Chansamouth, V., Chaurasia, S., Chiurchiù, S., Chowdhury, F., Clotaire Donatien, R., Cook, A.J., Cooper, B., Cressey, T.R., Criollo-Mora, E., Cunningham, M., Darboe, S., Day, N.P.J., De Luca, M., Dokova, K., Dramowski, A., Dunachie, S.J., Duong Bich, T., Eckmanns, T., Eibach, D., Emami, A., Feasey, N., Fisher-Pearson, N., Forrest, K., Garcia, C., Garrett, D., Gastmeier, P., Giref, A.Z., Greer, R.C., Gupta, V., Haller, S., Haselbeck, A., Hay, S.I., Holm, M., Hopkins, S., Hsia, Y., Iregbu, K.C., Jacobs, J., Jarovsky, D., Javanmardi, F., Jenney, A.W.J., Khorana, M., Khusuwan, S., Kissoon, N., Kobeissi, E., Kostyanev, T., Krapp, F., Krumkamp, R., Kumar, A., Kyu, H. H., Lim, C., Lim, K., Limmathurotsakul, D., Loftus, M.J., Lunn, M., Ma, J., Manoharan, A., Marks, F., May, J., Mayxay, M., Mturi, N., Munera-Huertas, T., Musicha, P., Musila, L.A., Mussi-Pinhata, M.M., Naidu, R.N., Nakamura, T., Nanavati, R., Nangia, S., Newton, P., Ngoun, C., Novotney, A., Nwakanma, D., Obiero, C.W., Ochoa, T.J., Olivas-Martinez, A., Olliaro, P., Ooko, E., Ortiz-Brizuela, E., Ounchanum, P., Pak, G.D., Paredes, J.L., Peleg, A.Y., Perrone, C., Phe, T., Phommasone, K., Plakkal, N., Ponce-de-Leon, A., Raad, M., Ramdin, T., Rattanavong, S., Riddell, A., Roberts, T., Robotham, J.V., Roca, A., Rosenthal, V.D., Rudd, K.E., Russell, N., Sader, H.S., Saengchan, W., Schnall, J., Scott, J.A.G., Seekaew, S., Sharland, M., Shivamallappa, M., Sifuentes-Osornio, J., Simpson, A.J., Steenkeste, N., Stewardson, A.J., Stoeva, T., Tasak, N., Thaiprakong, A., Thwaites, G., Tigoi, C., Turner, C., Turner, P., van Doorn, H.R., Velaphi, S., Vongpradith, A., Vongsouvath, M., Vu, H., Walsh, T., Walson, J.L., Waner, S., Wangrangsimakul, T., Wannapinij, P., Wozniak, T., Young Sharma, T.E.M.W., Yu, K. C., Zheng, P., Sartorius, B., Lopez, A.D., Stergachis, A., Moore, C., Dolecek, C., Naghavi, M., 2022. Global burden of bacterial antimicrobial resistance in 2019: a systematic analysis. The Lancet (london, England) 399, 629–655.

Mähler Convenor, M., Berard, M., Feinstein, R., Gallagher, A., Illgen-Wilcke, B., Pritchett-Corning, K., Raspa, M., 2014. FELASA recommendations for the health monitoring of mouse, rat, hamster, guinea pig and rabbit colonies in breeding and experimental units. Lab. Anim 48, 178–192.

Nielsen, R.B., Holm, R., Pijpers, I., Snoeys, J., Nielsen, U.G., Nielsen, C.U., 2021. Oral etoposide and zosuquidar bioavailability in rats: Effect of co-administration and in vitro-in vivo correlation of P-glycoprotein inhibition. INT J PHARM-X 3, 100089.

Nielsen, R.B., Larsen, B.S., Holm, R., Pijpers, I., Snoeys, J., Nielsen, U.G., Tho, I., Nielsen, C.U., 2023. Increased bioavailability of a P-gp substrate: Co-release of etoposide and zosuquidar from amorphous solid dispersions. Int. J. Pharm. 642, 123094.

O'Neill, J., 2016. Review on antimicrobial resistance: tackling drug-resistant infections globally: final report and recommendations. London, UK, Wellcome Trust, pp. 2–5.

Oostendorp, R.L., Huitema, A., Rosing, H., Jansen, R.S., ter Heine, R., Keessen, M., Beijnen, J.H., Schellens, J.H.M., 2009. Coadministration of Ritonavir Strongly Enhances the Apparent Oral Bioavailability of Docetaxel in Patients with Solid Tumors. Clin. Cancer Res. 15, 4228–4233.

Owen, D.R., Allerton, C.M.N., Anderson, A.S., Aschenbrenner, L., Avery, M., Berritt, S., Boras, B., Cardin, R.D., Carlo, A., Coffman, K.J., Dantonio, A., Di, L., Eng, H., Ferre, R., Gajiwala, K.S., Gibson, S.A., Greasley, S.E., Hurst, B.L., Kadar, E.P., Kalgutkar, A.S., Lee, J.C., Lee, J., Liu, W., Mason, S.W., Noell, S., Novak, J.J., Obach, R.S., Ogilvie, K., Patel, N.C., Pettersson, M., Rai, D.K., Reese, M.R., Sammons, M.F., Sathish, J.G., Singh, R.S.P., Steppan, C.M., Stewart, A.E., Tuttle, J. B., Updyke, L., Verhoest, P.R., Wei, L., Yang, Q., Zhu, Y., 2021. An oral SARS-CoV-2 M^{pro} inhibitor clinical candidate for the treatment of COVID-19. Science 374, 1586–1593.

Pandi, P., Bulusu, R., Kommineni, N., Khan, W., Singh, M., 2020. Amorphous solid dispersions: An update for preparation, characterization, mechanism on bioavailability, stability, regulatory considerations and marketed products. Int. J. Pharm. 586, 119560.

Paukner, S., Riedl, R., 2017. Pleuromutilins: Potent Drugs for Resistant Bugs-Mode of Action and Resistance. Cold Spring Harbor Perspectives in Medicine 7.

Petersen, E.F., Larsen, B.S., Nielsen, R.B., Pijpers, I., Versweyveld, D., Holm, R., Tho, I., Snoeys, J., Nielsen, C.U., 2024. Co-release of paclitaxel and encequidar from amorphous solid dispersions increase oral paclitaxel bioavailability in rats. Int. J. Pharm. 654, 123965.

Poulsen, S.M., Karlsson, M., Johansson, L.B., Vester, B., 2001. The pleuromutilin drugs tiamulin and valnemulin bind to the RNA at the peptidyl transferase centre on the ribosome. Mol. Microbiol. 41, 1091–1099.

Sankatsing, S.U., Beijnen, J.H., Schinkel, A.H., Lange, J.M., Prins, J.M., 2004. P glycoprotein in human immunodeficiency virus type 1 infection and therapy. Antimicrob. Agents Chemother. 48, 1073–1081.

Sevrioukova, I.F., Poulos, T.L., 2010. Structure and mechanism of the complex between cytochrome P4503A4 and ritonavir. Proc. Natl. Acad. Sci. 107, 18422–18427.

Sham, H.L., Kempf, D.J., Molla, A., Marsh, K.C., Kumar, G.N., Chen, C.-M., Kati, W., Stewart, K., Lal, R., Hsu, A., Betebenner, D., Korneyeva, M., Vasavanonda, S., McDonald, E., Saldivar, A., Wideburg, N., Chen, X., Niu, P., Park, C., Jayanti, V., Grabowski, B., Granneman, G.R., Sun, E., Japour, A.J., Leonard, J.M., Plattner, J.J., Norbeck, D.W., 1998. ABT-378, a Highly Potent Inhibitor of the Human Immunodeficiency Virus Protease. Antimicrob. Agents Chemother. 42, 3218–3224.

Tomaru, A., Takeda-Morishita, M., Banba, H., Takayama, K., 2013. Analysis of the Pharmacokinetic Boosting Effects of Ritonavir on Oral Bioavailability of Drugs in Mice. Drug Metab. Pharmacokinet. 28, 144–152.

Van den Mooter, G., 2012. The use of amorphous solid dispersions: A formulation strategy to overcome poor solubility and dissolution rate. Drug Discov. Today Technol. 9, e79–e85.

Vo, C.-L.-N., Park, C., Lee, B.-J., 2013. Current trends and future perspectives of solid dispersions containing poorly water-soluble drugs. Eur. J. Pharm. Biopharm. 85, 799–813.

Vogel, M., Rockstroh, J.K., 2005. Safety of lopinavir/ritonavir for the treatment of HIV-infection. Expert Opin. Drug Saf. 4, 403–420.

White, A., Hughes, J.M., 2019. Critical Importance of a One Health Approach to Antimicrobial Resistance. Ecohealth 16, 404–409.

World Health Organization, 2024. WHO Bacterial Priority Pathogens List, 2024. World Health Organization, Geneva.

Yan, K., Madden, L., Choudhry, A.E., Voigt, C.S., Copeland, R.A., Gontarek, R.R., 2006. Biochemical characterization of the interactions of the novel pleuromutilin derivative retapamulin with bacterial ribosomes. Antimicrob. Agents Chemother. 50, 3875–3881.

Zeitlinger, M., Schwameis, R., Burian, A., Burian, B., Matzneller, P., Müller, M., Wicha, W.W., Strickmann, D.B., Prince, W., 2016. Simultaneous assessment of the pharmacokinetics of a pleuromutilin, lefamulin, in plasma, soft tissues and pulmonary epithelial lining fluid. J. Antimicrob. Chemother. 71, 1022–1026.

Zeldin, R.K., Petruschke, R.A., 2004. Pharmacological and therapeutic properties of ritonavir-boosted protease inhibitor therapy in HIV-infected patients. J. Antimicrob. Chemother. 53, 4–9.

Zhanel, G.G., Deng, C., Zelenitsky, S., Lawrence, C.K., Adam, H.J., Golden, A., Berry, L., Schweizer, F., Zhanel, M.A., Irfan, N., Bay, D., Lagacé-Wiens, P., Walkty, A., Mandell, L., Lynch, J.P., Karlowsky, J.A., 2021. Lefamulin: A Novel Oral and Intravenous Pleuromutilin for the Treatment of Community-Acquired Bacterial Pneumonia. Drugs 81, 233–256.